Optics Letters

Ns-duration transient Bragg gratings in silica fibers

Avishay Shamir,[1] Aviran Halstuch,[1] Yonatan Sivan,[2] and Amiel. A. Ishaaya[1,*]

[1]Deptartment of Electrical and Computer Engineering, Ben-Gurion University of the Negev, Beer-Sheva 84105, Israel
[2]Unit of Electro-Optics Engineering, Faculty of Engineering Science, Ben-Gurion University of the Negev, Beer-Sheva 84105, Israel
*Corresponding author: ishaaya@bgu.ac.il

Received 6 July 2017; accepted 2 October 2017; posted 18 October 2017 (Doc. ID 301848); published 14 November 2017

We demonstrate, for the first time to our knowledge, fast all-optical switching in standard silica fibers, based on a transient Bragg grating. The grating is implemented in the fiber using an immunization photo-pretreatment process, followed by side illumination with femtosecond laser pulses through a suitable phase mask. Each pulse is nonlinearly absorbed, creating a thermal grating that is washed out by thermal diffusion. Reflections measured from such gratings are characterized by a very fast rise time, nanoseconds duration, and a high extinction ratio. © 2017 Optical Society of America

OCIS codes: (190.2055) Dynamic gratings; (060.3735) Fiber Bragg gratings; (130.4815) Optical switching devices; (060.4370) Nonlinear optics, fibers.

https://doi.org/10.1364/OL.42.004748

A fiber Bragg grating (FBG) is a periodic modulation of the refractive index in the core of an optical fiber. FBGs are used as key optical components in numerous applications, such as fiber laser mirrors, stress or temperature sensors, and add\drop multiplexers, and have also been considered for optical switching [1]. FBG switching typically involves shifting the Bragg wavelength away from the signal wavelength by introducing a disturbance to the grating. Several methods have been demonstrated by applying heat or stress, grating phase shifting, or nonlinear effects, such as cross-phase modulation induced on the grating or signal wavelength by a co-propagating pump pulse [2–4]. The schemes differ by the mechanism involved, which determines the switching speed and extinction ratio. More fundamentally, all of the above schemes rely on permanent gratings that correspond to a specific pre-determined signal wavelength.

The concept of transient (or dynamic) Bragg gratings refers to gratings that appear for a limited time and are used in various fields as measurement and characterization tools, typically in pump probe configurations [5]. Once a transient grating is formed, it exists only for a finite time duration, after which the grating is "erased." There are several mechanisms that can be exploited in order to form a short-duration transient Bragg grating. One mechanism is the Kerr effect, whereby the refractive index is intensity dependent. Here, a high-power, periodically structured (spatially), ultrashort pump pulse induces a transient periodic change in the refractive index of the material, forming a spatial grating, which is limited in time to the pump pulse duration. Another mechanism, which is suitable in semiconductors, is periodic excitation of free carriers that results in a strong periodic modulation of the refractive index. In this case, the grating will be washed out once the free carriers have diffused enough (one period of the spatial grating) [6,7]. Finally, the refractive index also depends on temperature, so a mechanism in which a periodic temperature grating is induced in the material will also form a transient grating. Transient Kerr gratings have been used for chemistry and spectroscopy [8], and for the study of free carrier dynamics in semiconductors [9]. Furthermore, they have been used for optical parametric conversion, and were suggested, theoretically, for optical switching [10–12]. Transient thermal gratings are used, among others, to measure the diffusion coefficient of materials [13].

To the best of our knowledge, short duration transient Bragg gratings have not been realized in the important platform of silica optical fibers. However, other transient phenomena in fibers have been investigated, both numerically and in experiments. Dynamic population gratings in active fibers were implemented via counter propagating waves, and resulted in milli-seconds (ms) time responses [14]. Transient gratings, a few cm long, were implemented using 193 nm, nanosecond (ns) excimer laser pulses and a 3 cm first-order, phase mask in phosphosilicate fibers without hydrogen loading. In passive fibers, reflection of tens of seconds duration was demonstrated [15], while in active fibers, the grating was based on population inversion, and the time response was estimated to be ms long [16].

Transient grating-based switching was suggested numerically by coupling light from the fundamental mode to high-order modes [17]. Ns switching was implemented using the Kerr effect with a highly nonlinear polymer layer deposited close to the core of a polished fiber [18]. It was suggested, theoretically, that a transient Bragg grating would result in an ultrafast switching response [19]. Thermal phenomena are typically associated with relatively long (μs) time scales. Recently, it was suggested, theoretically, that picosecond scale switching is achievable with thermal gratings, using metal nanoparticles in waveguides [20]. Ns switching of a permanent FBG was demonstrated by introducing electrodes into a special two-hole fiber [21]; however, this device suffers from ns rise time and ms time scale to return to its original state.

In this Letter, we experimentally demonstrate ns-duration transient thermal gratings inside standard silica single-mode

fiber (SMF), using side-illumination with femtosecond (fs) laser pulses, and investigate their switching characteristics in terms of the pulse energy and repetition rate of the illuminating fs pulse. A fs laser pulse is launched through a phase mask to create a periodic light structure along the fiber core. The high-peak intensity in this periodic structure leads to multi-photon nonlinear absorption [22], causing a periodic heat distribution along the fiber. The resulting thermal grating is characterized by an ultrafast rise time and ns-scale relaxation time. We managed to demonstrate this transient grating with negligible permanent effects; hence, the switching can be repeatedly accomplished at the same place. The Bragg wavelength of the transient grating can be adapted to any optical wavelength by changing the phase mask, and it delivers a high extinction ratio, as no signal is reflected when the grating is not present. As opposed to previous work with UV excimer lasers [15,16], we show ns transient grating in passive silica fiber, several orders of magnitude improvement in terms of grating duration. Our technique is based on nonlinear absorption, rather than linear UV absorption, generating a temperature grating within the fiber core, and thus is applicable to both passive and active fibers. Compared to previous work, our transient gratings show faster switching times in standard passive fiber, with a different physical mechanism.

Our experimental setup is shown in Fig. 1. The inscribing laser is a 1 kHz Ti:sapphire amplified fs system (Coherent Legend Elite) with 3.5 mJ and 35 fs pulses at a central wavelength of 800 nm. The beam diameter is 8.5 mm and has a Gaussian profile. The beam is attenuated and focused with a 40 mm cylindrical lens on the core of a jacket-striped SMF-28 fiber. A periodic light structure is formed with a phase mask that is placed between the cylindrical lens and the fiber. The phase mask (IBSEN Ltd.) has a pitch of 2140 nm, suitable for a Bragg wavelength of 1548.5 nm (2nd order) with less than 4% power in the zero order. The phase mask is positioned 1.9 mm away from the fiber to ensure pure two-beam interference [23]. Our signal laser is composed of a fiber-coupled distributed feedback laser (DFB) continuous-wave (CW) laser diode at 1550 nm wavelength, spliced to two fiber amplification stages. By controlling the DFB temperature, we could tune the signal wavelength slightly. The output power of the amplified signal source is 900 mW. If the Bragg wavelength of our transient grating is beyond the tuning range of the signal laser, we use a low-power spherical lens that is mounted on the phase mask to slightly shift the Bragg wavelength. The tuning lens has a focal length of 1200 mm and can be used to obtain a shift of several nm to the Bragg wavelength [24].

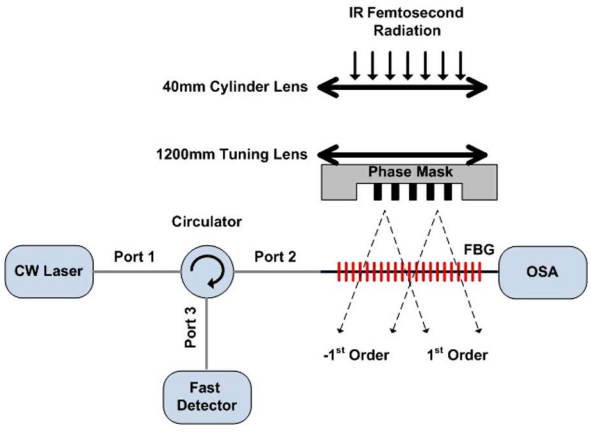

Fig. 1. (Color online.) Experimental setup.

Before the experiment, we apply an "immunization" procedure, as described in [25]. We scan the fiber 20 μm around the fiber core, in a direction perpendicular to the fiber and the optical axis of the pump beam, with a uniform line pattern (8.5 mm × 6 μm) and 1 mJ pulse energy ($\sim 6 \cdot 10^{13}$ W/cm^2) for 1.2 M pulses. This induces an elevated (uniform) refractive index level in the fiber core and its surroundings, up to a saturation point. This procedure results in an increase in the permanent inscription threshold, which enables us to increase the pump pulse power in the transient experiments with negligible permanent inscription effects. During the procedure, we removed the phase mask and the tuning lens, and reinstalled them at the end of the process. Once the immunization process is complete, we illuminate the fiber core with fs pulses, inducing gratings, and measure signal reflections from them with a fast photodiode (Thorlabs DET08CFC; 70 ps rise time) and a LeCroy DDA-120 oscilloscope.

The theory of a sinusoidal temperature grating is outlined in detail in Ref. [5]. Here, we shortly present the final results to provide the context for this work. The diffusion equation for a temperature grating can be divided into a temperature grating part and an average temperature part. The grating equation has an analytical solution when the initial temperature distribution (as induced, in our case, by the absorption of the pump beam) is composed of rectangular pulses or short spikes, or is periodically modulated. For short spikes, as in our case,

$$\Delta T_g(t) = \Delta T_g(t_p) e^{-\frac{t}{\tau_q}} \qquad \text{for } t > t_p. \tag{1}$$

Here, $\Delta T_g(t)$ is the temperature grating amplitude. $\tau_q = 1/(D_{\text{th}} q^2)$ is the thermal diffusion time constant that depends on the thermal diffusivity D_{th} and the grating vector $q = 2\pi/\Lambda_g$, where Λ_g is the grating period. Assuming a thermal diffusivity of $8.5 \cdot 10^{-7}$ m^2/s at room temperature for fused silica [26], and a grating period of 1070 nm, the expected temperature (and refractive index) diffusion time constant is 34 ns. Thus, by generating temperature gratings within the fiber, we should be able to generate ns pulses with ultrafast rise times.

After completing the photo-treatment process on a standard SMF, the laser pulse rate was lowered to 2 Hz in order to reduce the average thermal effects, and reflected pulses were measured with the photo diode. The amplified DFB signal wavelength was at 1547.6 nm. Figure 2 (left) shows the averaged time trace (100 pulses) of the reflected pulse for different fs illumination pulse energies (all below half of the immunization pulse energy).

As is evident, the reflected pulse has a very fast rise time followed by a relatively slow (ns) decay. The observed transient increase in the reflectivity can mainly be attributed to local heating of the silica, due to nonlinear absorption, corresponding to a local increase in the refractive index, and is followed by thermal diffusion that washes out the grating. This is corroborated by the very fast rise time of the reflected pulse, and the slow decay typical of thermal diffusion at these sizes and distances. The measured rise time is 2 ns, but we believe the actual rise time is significantly shorter, since our measurement was limited by our detection system (about the same rise time was also measured for our 35 fs laser source). For a 550 μJ illumination pulse, the reflected pulse duration is approximately 14.3 ns (measured between 1/e points). An exponential fit is shown (light blue) in Fig. 2 (left), with a time constant of ~10 ns.

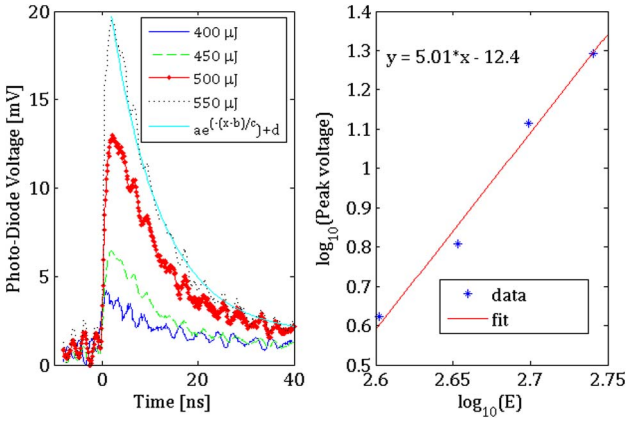

Fig. 2. (Color online.) (Left): Measured average time trace of reflected pulses for different fs illumination pulse energies. The illuminating pulse rate was 2 Hz. An exponential fit with parameters: $a = 17.87$, $b = 2.06$, $c = 10.5$, and $d = 1.7$ is shown for the highest reflectivity, indicating a thermal diffusion time of ~10 ns. (Right): Peak amplitude of the reflected signal as a function of pulse energy. The fit indicates a nonlinear relation between the pulse energy and reflectivity.

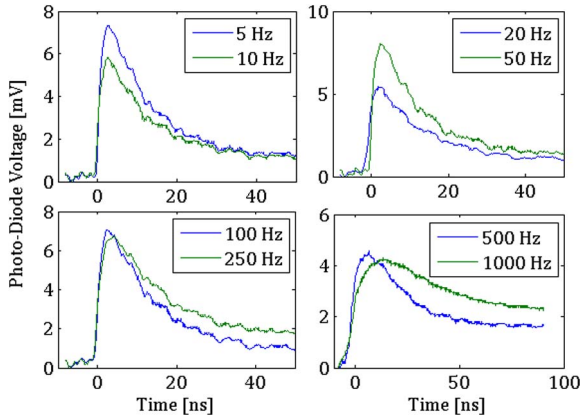

Fig. 3. (Color online.) Measured time traces of reflected pulses for different illuminating pulse rates. The illuminating pulse energy was 450 μJ. The results are averaged over 1000 pulses for 5 Hz–20 Hz, over 4000 pulses for 50 Hz, and over 10 k pulses for higher pulse rates. The DFB wavelength signal source was fixed throughout the experiments.

For a 550 μJ illumination pulse, the measured reflected peak power is 0.38 mW, according to the detector responsivity and oscilloscope 50 Ω coupling (the input CW power of our DFB signal was 900 mW). This corresponds to a reflectivity of 0.0435%.

Assuming an effective grating length of 5 mm, and applying the theory for spatial-temporal gratings [19], we estimate an index change of $n = 2.3 \cdot 10^{-6}$. This is three orders of magnitude less than reported in the literature for permanent fs inscribed gratings. However, it should be noted that tens of thousands of pulses are used to achieve the reported Δn for permanent inscription. The efficiency may be improved with higher pulse energies, different pump wavelengths suitable for 10-photon absorption, for example, or fibers with higher nonlinearity. The reflected power from a temporal grating is proportional to $(\Delta n)^2$; thus, we expect from theory a reflected signal decay time of 17 ns. This is in good agreement with the experimental results, in which differences may arise due to the presence of germanium.

A small increase in the inscribing pulse energy results in a higher induced transient refractive index change, leading to a significantly stronger reflected pulse. Figure 2 (right) shows the log of the peak reflected signal as a function of the illumination pulse energy. As suggested by the linear fit, the peak reflectivity has, indeed, a nonlinear growth that corresponds to I^5, which is a good indication that the grating is, indeed, based on multiphoton absorption. As the intensity depends on the square of the electric field, and the reflected power depends on the square of the induced index, the same relation applies for Δn—*Electric field*.

Next, we examine the effect of higher illuminating pulse rates on the reflected pulse shape. Figure 3 shows the average reflected pulse shapes for different illuminating pulse rates at a constant inscription pulse energy of 450 μJ. The reflected pulse time traces are similar below 500 Hz. The reflected pulse amplitude is as observed for a low repetition rate of 2 Hz; however, the pulse-to-pulse variations are larger at higher repetition rates. This could be the result of an increase in the average uniform index change term of the temperature grating, which causes contrast reduction and a slight shift in the wavelength.

The pulse duration slightly increases for higher rates, from ~14.3 ns at 5 Hz to ~20 ns at 250 Hz. For 500 Hz and higher, a different behavior is observed. The measured pulse durations are more than 50 ns, where a long tail (not shown in the figure) extends to the μs time scale. Note that for 500 Hz, two time scales are present—a fast reflectivity decrease in the first 50 ns, followed by a long tail, while for 1 kHz, no fast decrease is observed.

We found that by slightly tuning our signal wavelength, we could compensate the effects observed at high repetition rates (the longer pulse duration and the tail). The measured time traces of the reflected pulses as a function of the input DFB signal wavelength at an illuminating pulse rate of 1 kHz, is shown in Fig. 4. The reflected pulse duration is reduced by tuning the signal wavelength. The pulse duration decreases back to ~20 ns for an input signal wavelength of ~1549 nm. We note here that beyond 1549.06 nm, no reflected signal was observed, either because the reflected signal was too weak or because for these conditions, the signal wavelength is beyond the thermal Bragg shift. The relatively large tuning range of the DFB (~1 nm) is typical for transient gratings due to the low index contrast and the non-uniform profile (e.g., Ref. [15], who reported 0.6 nm bandwidth for 3 cm long grating).

The measured reflections are affected by both the average thermal shift and the grating bandwidth. As the signal wavelength increases, it matches better the effective thermal Bragg grating wavelength. The refractive index dependency on the temperature is approximately $10 \cdot 10^{-6}$ [K^{-1}] [27]. Our index change of $\sim 2 \cdot 10^{-6}$ thus corresponds to a temperature rise of ~0.2 K at a low pulse rate (e.g., 2 Hz), and a shift of 1 nm (at 1 kHz) corresponds to an average temperature increase of ~100 K, based on the temperature dependent index change.

Similar μsec time scale responses, as observed for 500 Hz and 1 KHz, were measured in different experiments, in which a Bragg wavelength of a permanent grating sweeps the DFB wavelength due to a thermal transient. Therefore, we conjugate that a small permanent grating is formed during the

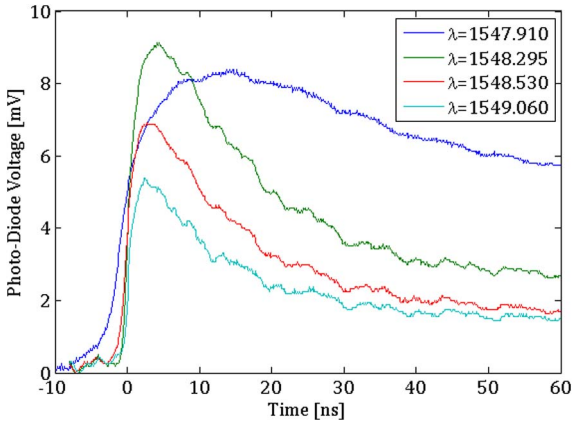

Fig. 4. (Color online.) Measured time trace of the reflected pulse for several input signal wavelengths. Every time trace is the average over 10 K pulses. The illuminating pulse energy was 450 μJ at a rate of 1 kHz.

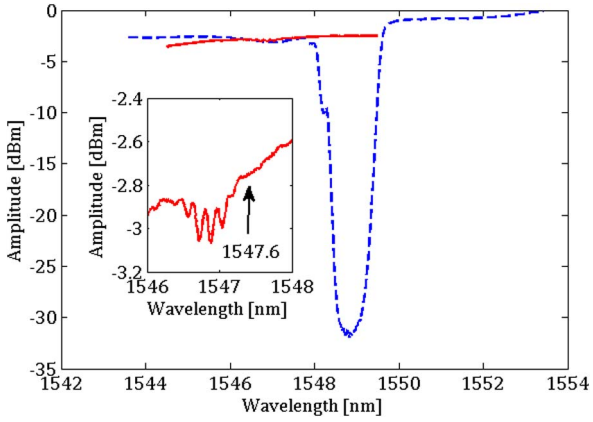

Fig. 5. (Color online.) Spectrum of the permanent FBGs measured at the end of the experiments (after 150 K pulses) with the fs laser pretreatment (solid red line) versus a typical grating without fs laser pre-treatment (150 K pulses, 180 μJ pulse energy; dashed blue line) taken from [25].

experiment, and that thermal shift of this grating is affecting the reflected signal.

During the experiments, we had illuminated the fiber core with a total of more than 150 K pulses, with pulse energies of 400–550 μJ at different rates. In Fig. 5, we show the measured spectral transmission curves [using an amplified spontaneous emission (ASE) signal source] of two different fibers that were illuminated, where one was not pre-treated and the other was the fiber that was pretreated and used in the experiments. For the fiber that had not undergone the preliminary photo treatment, a full 30 dB permanent grating is observed for such a number of illumination pulses. For the fiber we used in the experiments, we obtained only a weak 0.25–0.3 dB permanent grating. This means that the transient gratings resulted in negligible permanent grating inscription that adds a small DC background reflection (and may explain the behavior at high repetition rates).

To conclude, we have demonstrated, for the first time to the best of our knowledge, an in-fiber transient Bragg grating in the ns regime. The Bragg grating is mainly of thermal origin due to the relatively long time durations, which are in good correspondence with the decay time calculated for thermally excited gratings in silica. When increasing the repetition rate of the illuminating beam, we see effects of accumulated average heat, which causes a shift in the Bragg wavelength. Finally, the preliminary fs photo treatment significantly limits the formation of permanent inscription effects. Our results clearly indicate that a fs pulse can excite a transient grating with a very short rise time and ns time duration in a silica fiber. We believe this constitutes a first step in a different approach towards ultrafast optical switching in pure silica fibers.

Future work may focus on increasing the switching efficiency by illuminating with different wavelengths corresponding to two- or 10-photon absorption or by using different types of fibers with higher nonlinearity. Finally, use of first-order masks should lead to shorter duration and stronger transient gratings.

REFERENCES

1. R. Kashyap, *Fiber Bragg Gratings* (Academic, 1999).
2. S. Y. Li, N. Q. Ngo, S. C. Tjin, P. Shum, and J. Zhang, Opt. Lett. **29**, 29 (2004).
3. H. Uno, A. Kojima, A. Shibano, and O. Mikami, in *Optical Engineering for Sensing and Nanotechnology (ICOSN'99)* (International Society for Optics and Photonics, 1999), pp. 247–277.
4. I. V. Kabakova, D. Grobnic, S. Mihailov, E. C. Mägi, C. M. de Sterke, and B. J. Eggleton, Opt. Express **19**, 5868 (2011).
5. H. J. Eichler, P. Günter, and D. W. Pohl, *Laser-Induced Dynamic Gratings* (Springer, 1986), Vol. **50**.
6. H. J. Eichler and F. Massmann, J. Appl. Phys. **53**, 3237 (1982).
7. Y. Sivan, G. Ctistis, E. Yüce, and A. P. Mosk, Opt. Express **23**, 16416 (2015).
8. F. W. Deeg, J. J. Stankus, S. R. Greenfield, V. J. Newell, and M. D. Fayer, J. Chem. Phys. **90**, 6893 (1989).
9. A. Othonos, J. Appl. Phys. **83**, 1789 (1998).
10. J. Reif, R. P. Schmid, and T. Schneider, Appl. Phys. B **74**, 745 (2002).
11. H. Zoweil and J. W. Y. Lit, Opt. Commun. **212**, 57 (2002).
12. A. F. G. F. Filho, J. R. R. de Sousa, A. F. de Morais Neto, J. W. M. Menezes, and A. S. B. Sombra, J. Electromagn. Anal. Appl. **4**, 17667 (2012).
13. J. E. Graebner, Rev. Sci. Instrum. **66**, 3903 (1995).
14. S. Stepanov, J. Phys. D **41**, 224002 (2008).
15. J. Canning, M. G. Sceats, H. G. Inglis, and P. Hill, Opt. Lett. **20**, 2189 (1995).
16. J. Canning and M. G. Sceats, Electron. Lett. **31**, 576 (1995).
17. O. Akin and M. S. Dinleyici, J. Lightwave Technol. **28**, 3470 (2010).
18. O. Akin and M. S. Dinleyici, Opt. Lett. **39**, 1469 (2014).
19. Y. Sivan, S. Rozenberg, A. Halstuch, and A. A. Ishaaya, Sci. Rep. **6**, 29010 (2016).
20. J. B. Khurgin, G. Sun, W. T. Chen, W. Y. Tsai, and D. P. Tsai, Sci. Rep. **5**, 17899 (2015).
21. Z. Yu, W. Margulis, O. Tarasenko, H. Knape, and P. Y. Fonjallaz, Opt. Express **15**, 14948 (2007).
22. R. R. Gattass and E. Mazur, Nat. Photonics **2**, 219 (2008).
23. C. W. Smelser, D. Grobnic, and S. J. Mihailov, Opt. Lett. **29**, 1730 (2004).
24. C. Voigtländer, R. G. Becker, J. Thomas, D. Richter, A. Singh, A. Tünnermann, and S. Nolte, Opt. Mater. Express **1**, 633 (2011).
25. A. Shamir and A. A. Ishaaya, Opt. Lett. **41**, 765 (2016).
26. P. Combis, P. Cormont, L. Gallais, D. Hebert, L. Robin, and J. L. Rullier, Appl. Phys. Lett. **101**, 211908 (2012).
27. M. B. Reid and M. Özcan, Opt. Eng. **37**, 237 (1998).

132.72.48.181 {ts '2017-12-20 10:05:41'}